AIAA

AIAA-93-2027

Applying Design Principles to Fusion Reactor Configurations for Propulsion in Space

S. Carpenter
Lawrence Berkeley Laboratory
Berkeley, CA

M. Deveny
Independent
Corona, CA

N. Schulze
NASA Headquarters
Washington, DC

AIAA/SAE/ASME/ASEE
29th Joint Propulsion Conference and Exhibit
June 28-30, 1993 / Monterey, CA

APPLYING DESIGN PRINCIPLES TO FUSION REACTOR CONFIGURATIONS FOR PROPULSION IN SPACE

Scott A. Carpenter†
Lawrence Berkeley Laboratory (LBL)
Berkeley, California

Marc E. Deveny*
Independent
Corona, California

Norman R. Schulze§
National Aeronautics and Space Administration (NASA)
Washington, D.C.

Abstract

The application of fusion power to space propulsion requires rethinking the engineering-design solution to controlled-fusion energy. Whereas the unit cost of electricity (COE) drives the engineering-design solution for utility-based-fusion-reactor configurations; (1) initial mass to low earth orbit (IMLEO), (2) specific jet power (kW_{thrust}/kg_{engine}), and (3) reusability drive the engineering-design solution for successful application of fusion power to space propulsion. We applied three design principles (DPs) to adapt and optimize three candidate-terrestrial-fusion-reactor configurations for propulsion in space. The three design principles are: (1) provide maximum direct access to space for waste radiation, (2) operate components as passive radiators to minimize cooling-system mass, and (3) optimize the plasma fuel, fuel mix, and temperature for best specific jet power. The three candidate-terrestrial-fusion-reactor configurations are: (1) the thermal-barrier-tandem-mirror (TBTM), (2) field-reversed-mirror (FRM), and (3) levitated-dipole-field (LDF). The resulting three candidate-space-fusion-propulsion systems have their IMLEO minimized and their specific jet power and reusability maximized. We performed a preliminary rating of these configurations and concluded that the leading engineering-design solution to space fusion propulsion is a modified TBTM that we call the Mirror Fusion Propulsion System (MFPS).

Nomenclature

DP	design principle
FRM	field-reversed-mirror reactor
LDF	levitated-dipole-field reactor
MCF	magnetic-confinement-fusion
MFPS	Mirror Fusion Propulsion System
NBI	neutral beam injection
RFTP	reversed-field theta-pinch
SGL	solar-gravity-lens mission
SM	simple-mirror reactor
TM	tandem-mirror reactor
TBTM	thermal-barrier-tandem-mirror reactor
n	neutron
p,d,t	ionized hydrogen isotopes, in the plasma
P,D,T	hydrogen isotopes, in the fuel pellet
$^{3,4}He$	helium isotopes
$^{6,7}Li$	lithium isotopes
^{9}Be	beryllium-9 isotope
^{11}B	boron-11 isotope
M	represents a light "metal" ($^{6,7}Li$ or ^{9}Be)
FF	fuel-fuel fusion reactions
FP	fuel-product fusion reactions
PP	product-product fusion reactions
L(p)	plasma-core length
r(p)	plasma-core radius
$<\beta>$	average plasma-core beta
$\%P_{AFT}$	Percent-power-available for thrust
Ti	ion temperature, Maxwellian distribution
Te	electron temperature, Maxwellian distribution
P_{FUS}	total fusion power
P_{Brem}	Bremsstrahlung (X-ray) power
P_{syn}	synchrotron power absorbed in the 1st wall
P_{χ}	transport power absorbed in the 1st wall
P_n	neutron-radiation power
B	magnetic field strength in Tesla
"s"	number of internal ion gyroradii in r_s
r_s	separatrix radius
l_s	separatrix length

† Senior Research Associate, Earth Sciences Division.
* Aerospace Engineer, Member, AIAA.
§ Aerospace Engineer, Independent.

Introduction

We demonstrate that contemporary utility-based-fusion-reactor configurations are inappropriate for space propulsion due to design-driver differences between terrestrial and space environments; however, through application of certain design principles, modifications to contemporary designs can result in appropriate space-fusion-propulsion configurations.

In Part 1, we describe basic information relevant to space fusion propulsion (e.g., choosing the fuel, its fuel mix, and its operating temperature). We discuss characteristics that affect these choices (e.g., side fusion reactions and four primary plasma radiations). To sort through all of these choices, and others, we describe three primary design principles that help us to make the correct choices. In Part 2, we give three examples of application of the three design principles to adapt, and then optimize, candidate-fusion-reactor configurations for propulsion in space. In Part 3, we demonstrate the improved mission performance of one of the three examples, the Mirror Fusion Propulsion System (MFPS), over contemporary proposed propulsion systems which include chemical (cryogenic), nuclear thermal (solid and gas core), and nuclear electric (20, 50, 100, and 200 MWe) for a hypothetical human-piloted Mars-exploration mission of 90-90-90-day duration. IMLEO and mission window are compared. We also characterize MFPS's ability to complete selected outer-solar-system missions and one specific extra-solar-system mission called the solar-gravity-lens (SGL) mission. In Part 4, we submit that it is both feasible and reasonable to propose and intensify studies of fusion power as applied to space propulsion, and that initially, these can be performed for minimal cost.

Part 1
Magnetic-Confinement-Fusion (MCF) Reactors, Fuels, Fuel-Mix, and Three Design Principles (DPs)

Nuclear fusion and nuclear fission are distinctly different processes. The nuclear fission process releases nucleon binding energy by splitting the largest of nuclei; e.g., uranium-235 and plutonium-239. Nuclear fission power sources are solid fuels contained in a ceramic and metal matrix, although liquid and gaseous cores have been proposed for use in space propulsion.[1,2] Nuclear fission is an established power source for propulsion (submarines and surface ships) and electrical power production (nuclear power plants).

In the nuclear fusion process, nucleon binding energy is released by combining very light nuclei; e.g., hydrogen-2 (deuterium), hydrogen-3 (tritium) and helium-3. In magnetic confinement, the reacting fuel particles are temporarily trapped on magnetic field lines produced by powerful superconducting magnets. The trapped particles form a tenuous plasma much thinner than air. Unlike nuclear fission, there are no operational nuclear fusion power plants, however there is an expanding experimental database containing concepts and principles validated at a variety of research centers around the world.[3] We shall consider only the magnetic-confinement-fusion (MCF) approach to controlling fusion. Nevertheless, the three design principles that we shall discussed apply to other approaches as well.

Magnetic-Confinement-Fusion (MCF) Reactors

MCF reactors fall into two main classes: "closed" and "open." Each of these classes entails great diversity, but there is one fundamental difference: in the closed class (Figure 1-1), the magnetic field lines and plasma remain trapped inside a mechanical device (the fusion reactor) whereas in the open class (Figure 1-2) the magnetic field lines, and a little plasma, escape beyond the confines of the physical reactor. In both classes, the plasma ions tend to "stick" to the magnetic field lines. These magnetic field lines protect the fusion reactor by keeping the bulk of the hot plasma away from the walls and hold enough of the plasma-fuel particles together for fusion to occur.

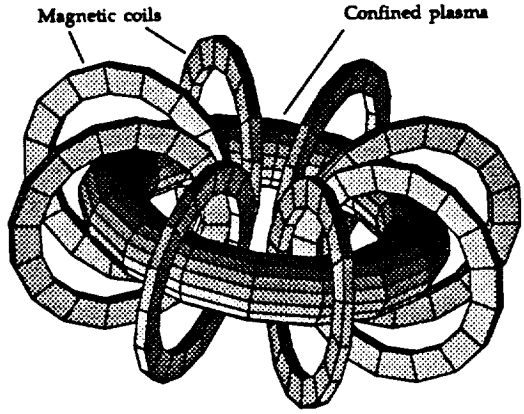

Figure 1-1. "Closed" magnetic-confinement example.

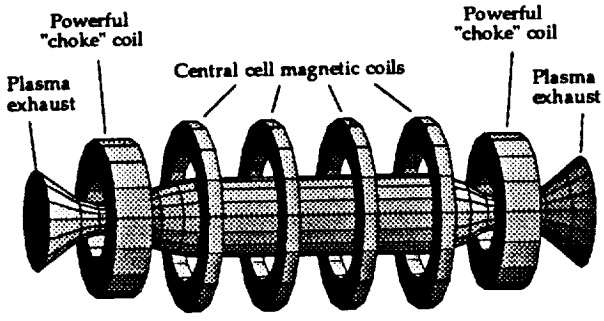

Figure 1-2. "Open" magnetic-confinement example.

We propose that the most reasonable magnetic configuration usable as a space-fusion-propulsion system is the open-magnetic-field geometry.[4,22,23] The open-magnetic-field geometry provides a natural

flow path for the hot plasma to heat a propellant and provide moderate thrusts at very high specific impulse (10,000 to 100,000 sec), or relatively small thrusts at ultra-high specific impulse[5] (>100,000 to 1,000,000 sec).

Fuels and Fuel Mix

Most candidate fusion fuels mentioned in the literature[6,7,8,36] for use in space propulsion fall into two distinct groups, the protium- and deuterium-based, and are listed in Table 1-1. The protium-based plasmas are known for their minimal neutron-producing state. The deuterium-based plasmas are known for their high probability for fusion reaction at relatively low temperatures (<100 keV).

Table 1-1. Candidate fusion fuels for use in space.

Protium-based fuels	Deuterium-based fuels
P^6Li	DT
P^9Be	DD
$P^{11}B$	D^3He

Side reactions. All of these fuels produce side fusion reactions. For example, in a d^3He plasma, all ten of the fusion reactions listed in Table 1-2 take place in tandem. To keep track of the relevant side reactions, we categorized them into three groups:

- fuel-fuel (FF) thermal reactions,
- fuel-product (FP) super-thermal reactions, and
- product-product (PP) super-thermal reactions.

Fuel-pellet injection controls the fuel-ion densities, which are usually the ions of highest density and reaction cross-section at plasma equilibrium conditions and therefore produce the larger fraction of the fusion power in fuel-fuel (FF) fusion reactions. As fuel pellets penetrate into the plasma, they rapidly ionize and come to thermal equilibrium in a near-Maxwellian distribution of particles with a mean temperature of, say, 90 keV (~1 billion °C). Fusion takes place, releasing fusion-product ions which may also be fusionable in fuel-product (FP) reactions (e.g., the dd reaction [2] of Table 1-2 produces a charged particle, the triton, which may fuse with the injected deuterium nuclei, Reaction [5]), and to a lesser extent, may also interact with themselves in product-product (PP) fusion reactions (e.g., Reactions [9] and [10]). Fusion-product ions have high kinetic energy in the hundreds or thousands of keV, hence super-thermal. This kinetic energy is distributed among the radiation terms (to be described shortly) and the bulk-plasma ions. The super-thermal reactions are often called "catalyzed" reactions because, in general, they have larger fusion-reaction cross-sections at their elevated super-thermal temperatures and burn more efficiently. Their most pronounced influence occurs in the DD-fueled fusion reactor. We conservatively assume that all fusion byproducts thermalize (come to equilibrium temperature with the bulk plasma) prior to fusing.

Table 1-2. d^3He fusion reactions[9,10] (energy in keV).

Fuel-Fuel (FF) fusion reactions			
d^3He	--->	p (14681) + ^4He (3670)	[1]
dd	--->	p (3024) + t (1008)	[2]
dd	--->	n (2450) + ^3He (817)	[3]
$^3He^3He$	--->	p (5716)+ p (5716) + ^4He (1429)	[4]
Fuel-Product (FP) fusion reactions			
dt	--->	n (14069) + ^4He (3517)	[5]
t^3He	--->	d (9546) + ^4He (4773)	[6]
t^3He	--->	n (5374) + p (5374) + ^4He (1344)	[7]
t^3He	--->	p (10077) + n (1612) + ^4He (2015)	[8]
Product-Product (PP) fusion reactions			
tt	--->	n (5034) + n(5034) + ^4He (1259)	[9]
pt	--->	n (-573) + ^3He (-191)	[10]

Primary plasma radiations. All of these candidate plasma-fuels produce four primary radiations resulting in un-usable power (although the $p\text{-}^{11}B$ plasma is extremely neutronless below 500 keV temperatures[10]). These four plasma radiations are:

- Bremsstrahlung (X-ray),
- synchrotron (microwave),
- neutron, and
- plasma transport.

The fusion process converts nuclear binding energy to product-particle kinetic energy. These particles are either positively-charged nuclei or neutrons. The neutrons immediately leave the plasma, being unaffected by the magnetic field, and may interact with engine components in their path. The charged particles immediately distribute their power to Bremsstrahlung and synchrotron radiation, and to a lesser extent, plasma transport to the walls of the reactor chamber. The remaining charged-particle kinetic energy is distributed among all the plasma particles and the power that remains available for thrust is:

$$P_{AFT} = P_{FUS} - P_{Brem} - P_{syn} - P_{\chi} - P_n \qquad (1.1)$$

Furthermore, in our calculation of specific jet power we have arbitrarily assumed that 20% of the P_{AFT} is lost to plasma neutralization and magnetic exhaust nozzle inefficiencies.

$$\text{Sp. Jet Power}\left(\frac{kW_{thrust}}{kg_{engine}}\right) = \frac{0.8\,(P_{AFT})}{M_{engine}} \qquad (1.2)$$

The engine mass (M_{engine}) includes the fusion engine and all of the subsystems required for normal operation, e.g., the radiator panel, piping, and coolant masses.

To determine the potential usefulness for space propulsion of the candidate fusion fuels (Table 1-1), we compared these fuels to each other as a function of fuel mix and temperature with the plasma ions and electrons in thermal equilibrium and Maxwellian in distribution. Figure 1-3 shows that only the deuteron-based fuels produce enough fusion power to overcome the plasma-cooling rate.

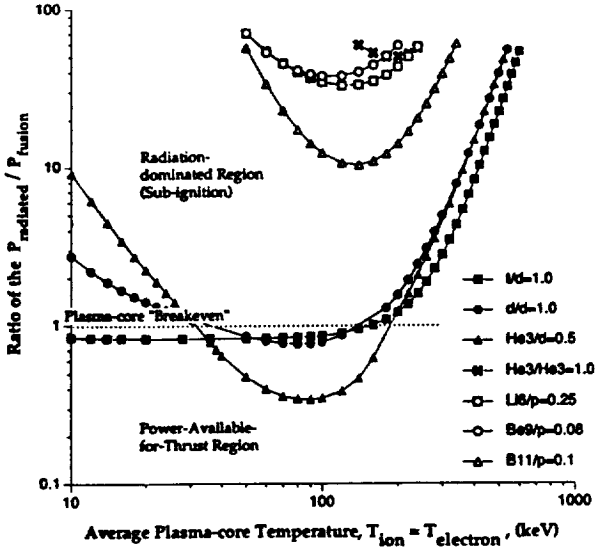

Figure 1-3. Fuel usefulness as a function of temperature and fuel mix.

The high cooling rate of the proton-based plasmas is primarily caused by electron-ion Bremsstrahlung. Bremsstrahlung is a strong function of electron temperature. In a real fusion reactor, the situation is likely to be better because it appears possible to operate these candidate-fusion-grade plasmas at hot ion temperatures (>100 keV) while holding the electron population lower in temperature, i.e., there will be less Bremsstrahlung (x-ray) radiation.

There remains a question as to how much lower than the ion temperature can the electron temperature be. To illustrate just how bad the problem is with the proton-based fuels, Figure 1-4 shows the improvement achieved in an imaginary plasma with a very cold electron population (0.1 keV). If the Bremsstrahlung can be minimized (by preventing the electrons from heating up) then the proton-based fuels, and a helium-3-based, produce more in-core power than un-usable radiation (as implemented in a proposed system,[11] MFPS, to be described further in Part 2).

Unfortunately, even if this imaginary cold-electron plasma could be achieved, proton-based-fuel use in space would still be doubtful because if implemented in a real device, e.g. MFPS, engineering concerns appear. Figure 1-5 shows the resultant magnetic field required to contain the individual plasmas (producing 4 GWt) within a 493.7 cubic meter cylindrical volume (MFPS central cell) and the resultant IMLEO at optimized specific jet power for MFPS. The large magnetic fields require larger superconducting coils, larger neutron and x-ray shields to protect these coils, and more massive structural members to control the magnetic forces.

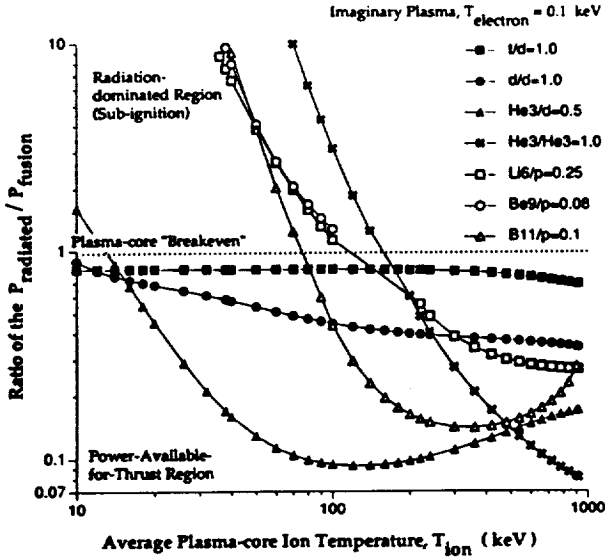

Figure 1-4. Proton and deuteron-based fuel performance for imaginary cold-electron plasmas in MFPS.

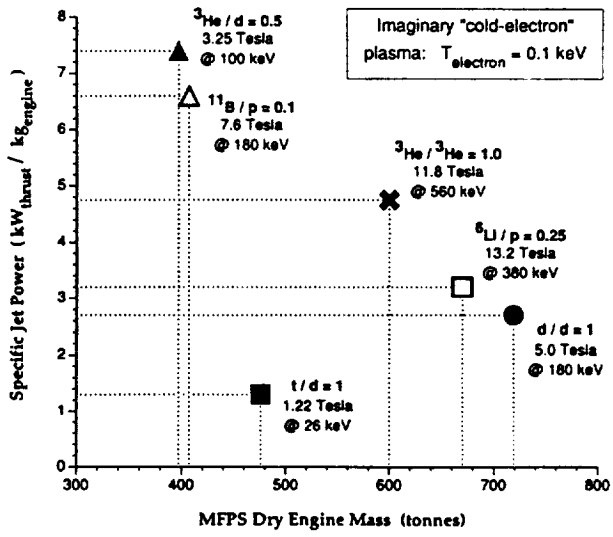

Figure 1-5. Comparison of imaginary cold-electron (0.1 keV) plasmas in MFPS, optimized for specific jet power.

Of academic interest under these imaginary circumstances is the $P^{11}B$-fueled plasma. At 180 keV, this protium-based fuel achieves nearly equal specific jet power and IMLEO as that for a $D^{3}He$-fueled plasma operating at 100 keV. This is due to the extreme aneutronicism of the p-^{11}B fusion reactions at the

relatively low 180-keV temperature. At this temperature, the neutron-shielding requirement is eliminated. However, structural mass increases to control higher magnetic fields for plasma containment.

For the remainder of our analysis, we assume the ions and electrons are in thermal equilibrium and Maxwellian in distribution.

Realistic Fusion Fuels for Space Propulsion. The primary problem with the protium-based fuels is their excessive Bremsstrahlung-emission rate. Of the deuterium-based fuels, D^3He appears to be the best for space-propulsion applications as shown in Figure 1-3. DT and DD produce a large percentage (~40 and 80% respectively) of their total fusion power in neutrons. However, the DD fuel shows promise as an emergency-backup fuel at lower, but still significant power operation[11] (~24% power available for thrust). However, power levels should be reduced (relative to D^3He operation) because of the high neutron flux from the DD and side reactions (Reactions [2], [3], and [5] in Table 1-2). The DT fuel may be useful during fusion engine startup, the plasma ignition phase, because of its relative ease to ignite at low temperatures (~10 keV). As the dt-plasma temperature increases, shelled D^3He pellets may be injected and the DT pellets phased out. On the negative side, 80% of the dt-fusion-reaction energy is released in neutron kinetic energy (Reaction [5] in Table 1-2).

Light-metal-shelling the "ideal" fuel (D^3HeM). It is desirable for space systems to use fuel-pellet injectors of minimal mass. Minimal mass implies compactness and short lengths for pellet acceleration. Short acceleration lengths translate into large stresses on the fuel pellet. On the basis of previous studies,[12,13] we assume pellet velocities between 10 and 30 km/s are achievable with very short acceleration lengths (< 10 m). However, a simple DD-ice shell is incapable of meeting the stress requirements.[14] Consequently, small amounts of a light metal (M) may be added to the "ideal" fuel, D^3He, to form a strong fuel pellet shell. Possible light-metal candidates that may satisfy this requirement include ^6Li, ^7Li, ^9Be, and possibly others.[15]

We envision encapsulating ^3He and D in a lithium deuteride (LiD), or beryllium (Be) metal shell for which we limit the Li or Be to a small atom percent (< 6 %). We have followed the degradation effects that these light metal ions have on our plasma and overall fusion-propulsion-system performance[11] (~6% overall reduction in power available for thrust when the light-metal ions in the plasma constitute < 6-atom percent). This degradation is due almost entirely to the Bremsstrahlung generated by the addition of the light-metal electrons: 3 electrons for each Li and 4 for each Be atom as compared to only 1 electron for each D and 2 for each ^3He atom.

Tables 1-3 and 1-4 list the useful fusion-fuel combinations considered in the remainder of this paper, with the electrons and ions in thermal equilibrium and Maxwellian in distribution when in the plasma state.

Table 1-3. Useful propulsion fuel combinations.

Ideal Fuel	Shelled-pellet Fuels
D^3He	D^3He^6Li D^3He^7Li D^3He^9Be

Table 1-4. Special-use fuels.

Start-up Fuel	Emergency Fuel
DT	DD

Three Design Principles (DPs)

We describe and demonstrate the importance of three design principles (DPs) for improving fusion-engine performance, and they are: (1) provide maximum direct access to space for waste radiation, (2) operate components as passive radiators to minimize cooling-system mass, and (3) optimize the plasma fuel, fuel mix, and temperature for best specific jet power.

DP-1: Maximize direct access to space for waste radiation. The primary-system-performance limiter is the waste heat absorbed by the engine. Between 30 and 50% of the total fusion power will be in waste heat. Minimizing the amount absorbed in the engine will allow higher total fusion power and specific jet power while minimizing engine component temperatures. We provide the waste heat with as much direct access to space as possible.

We use two methods to maximize direct access to space: (1) minimize components that surround the plasma and (2) use materials that present a small cross-section to the incoming x-ray and neutron radiation, thereby allowing the majority of those radiations to pass through the materials and into deep space.

DP-2: Operate components as passive radiators to minimize cooling-system mass. All space fusion propulsion systems will absorb some waste heat for which there are two general methods of removal: (1) provide a robust, massive active-cooling system or (2) operate as many components as possible in a passive cooling mode as a means to reduce the active-cooling-system mass. Option (2) is the better choice.

DP-3: Optimize the plasma fuel, fuel mix, and temperature for best specific jet power. We already demonstrated that D^3He is the fuel of choice in Figure 1-3. D^3He-contour regimes for percent-power-available for thrust vs. plasma temperature and ^3He-to-d fuel mix are shown in Figure 1-6. The thermodynamic optimal

operating point is about 90 keV and a plasma ^{3}He-to-d fuel mix of ~0.5; i.e., one helium-3 ion for two deuterium ions, giving a percent-power-available for thrust of ~65.8%. The power available for thrust represents the fusion power remaining as charged-particle kinetic energy that is delivered to the plasma-propellant-mixing region per second.

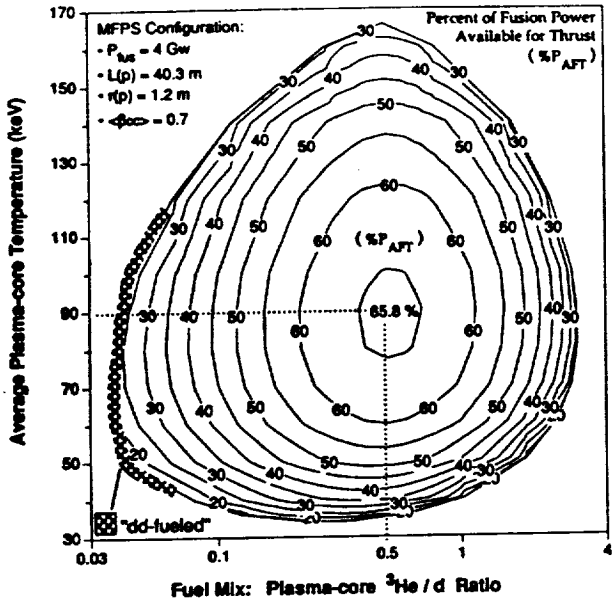

Figure 1-6. Contour regimes for percent-power-available for thrust ($\%P_{AFT}$).

This gives us our first estimate of the best plasma temperature and fuel mix to operate at. In Part 2, we shall show that the propulsion plant configuration makes the final determination.

If we chose a particular temperature to operate our plasma, say 90 keV, and study the impact of the four-primary-plasma radiations (Figure 1-7), we can gain insight into the engineering concerns that would result for a specific propulsion-plant configuration. In previous literature citations, the neutron-production rate in fuels has been over emphasized. Many authors have tried to reduce the neutrons at all (self-defeating) cost. For example, the d-^{3}He plasma produces neutrons that carry away between 1-to-45% of the total fusion power, depending primarily upon the plasma-ion fuel mix and temperature, T_i. However, Figure 1-7 demonstrates that to save a mere 1.4% in neutron power (moving from a fuel-mix of unity to 2.4), you must pay a 25% penalty in Bremsstrahlung (x-rays). These x-rays, like neutrons, immediately exit the plasma and interact with solid engine materials. Consequently, for a 1-GW-thermal fusion engine, to reduce neutron power by 14 MW, the fusion engine must absorb a 250-MW penalty in x-ray power, requiring an additional cooling system mass. All of these criteria (i.e., specific jet power, IMLEO, P_{AFT}, and others) are influenced further by the particular fusion reactor configuration and the specific space-propulsion-based engineering-design solution to that configuration. We discuss and quantify some of these influences in Part 2.

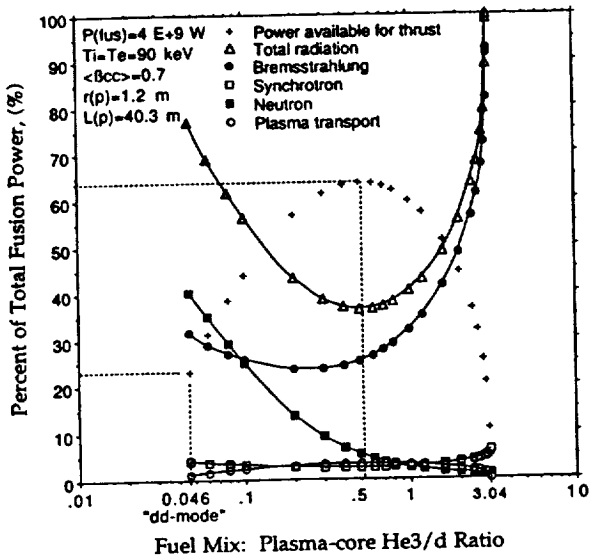

Figure 1-7. Percent power available for thrust @ 90 keV and ensuing plasma radiations. The endpoints in the lower left corner of the operating curves in Figure 1-7 represent pure-DD-fueled reactor operation. Even a plasma fueled by pure deuterium will always have helium-3 present in the plasma due to its production in the dd-side-fusion reaction (Reaction [3] in Table 1-2).

Part 2
Applying Design Principles (DPs) to Fusion-Reactor Configurations for Propulsion in Space

We describe application of three design principles to three candidate-terrestrial-fusion-reactor configurations that adapt them for propulsion in space, minimizing their IMLEO and maximizing their reusability and specific jet power. These three configurations are the (1) thermal-barrier-tandem-mirror (TBTM), (2) field-reversed-mirror (FRM), and (3) levitated-dipole-field (LDF).

(1) Thermal Barrier Tandem Mirror (TBTM) Config.

Magnetic-mirror machines for the purpose of controlling thermonuclear fusion reactions fall into three distinct evolutionary classes.[16] The earliest mirror machines were called simple mirrors[17] (SM). A breakthrough came in 1976 with development of the tandem mirror[18,19] (TM). And, in 1979, the electron thermal barrier[20] (TB) concept was added to the tandem mirror. We begin with a brief discussion of a "natural" magnetic mirror after which we shall describe each of the three mirror-machine classes in more detail.

Natural magnetic mirroring and basic mechanics. The principle of magnetic mirroring is a natural phenomenon and earth's Van Allen radiation belts are an excellent example.[21] As charged particles from the sun and space enter the influence of earth's magnetic field, they may become "trapped" on a magnetic-field line, allowed to move in a cork screw fashion around the field line that exits from one earth pole, loops out into space (where it caught the charged particle) and swings back to earth, entering at the opposite pole. The charged particle screws its way along the field line moving towards one of the earth's poles. Because all of the field lines are attempting to enter the earth at a relatively small location, the number of lines per unit area increases, i.e., an increasing magnetic field gradient, and the gyrating charged particle experiences a repelling force that can be described by the relation:

$$F = \mu(-\nabla B) \qquad (2.1)$$

where $\mu = \left(\frac{mv_\perp^2}{2} \cdot \frac{1}{B}\right)$ is the magnetic moment, ∇B is the magnetic field gradient, B is the strength of the magnetic field, m is the ion or electron mass, and $v_\perp$ is the charged-particle velocity perpendicular to B.

At the north and south poles, there is a net force opposite to the direction of motion of the gyrating charged particles that causes many to reverse their direction. It is as though they are trapped between two magnetic hills (north and south poles); thus, charged particles accumulate in the valley and form the Van Allen radiation belts.

Simple-mirror (SM). In the United States, one of the first experiments to demonstrate the plasma confining effect of magnetic mirrors took place in 1951 with the Post-Steller "simple" magnetic mirror device.[17] A simple mirror experimental setup is shown schematically in Figure 2-1(A). The two large coils (one on each end) produce stronger magnetic fields at the ends relative to the center, hence, a magnetic field gradient forms at the cylinder's throats that tends to reflect the particles - a magnetic mirror.

Unfortunately, in the simple-mirror machine much of the plasma is able to escape through the throats, and scaling up to a fusion power plant would result in an energy gain (Q) of ~1. That is to say, we would be lucky to get as much power from the machine as it takes to operate it. "Q" is a figure of merit related to the economy of fusion power plants and is defined as:

$$Q = \frac{\text{fusion power produced}}{\text{input power required to sustain fusion}} \qquad (2.2)$$

To approach economic viability, a commercial fusion power plant should have a Q > ~15. There are three primary reasons for low Q in the simple mirror. The first is that on each mirror pass, a fraction of the plasma (~ 10 %) has the required parallel kinetic energy to escape. The second is that a positive electrostatic potential develops in the central region. "Like" particles repel, and the positive potential provides an extra push on the particles that helps them escape from the fusion reactor. The third reason for low Q is the intangible "plasma instabilities" that can act as energy pumps, pushing the plasma out of the magnetic bottle at enhanced rates.

Tandem mirror (TM). To simultaneously overcome these three contributors to low Q, the tandem mirror reactor was invented independently by Dimov, et al.[18], in the Commonwealth of Independent States and Fowler and Logan[19] at the Lawrence Livermore National Laboratory (LLNL), USA. The tandem mirror concept, Figure 2-1(B), requires at least three linked magnetic-mirror cells. The two end mirror cells (called plug mirror cells) are each usually made from a set of coils or from a single coil that forms what is called a "minimum-B" geometry. By this we mean that a charged particle in the center of one of these plugs, upon moving in any direction feels increasing magnetic field, resulting in a stabilizing force.[24]

Plasma is introduced into all three mirror cells with the highest plasma density maintained in the plug mirror cells. The electrons in the plugs are deliberately heated to very high temperature. Being much lighter than ions, the electrons escape, leaving behind the ions. Very large positive electrostatic potentials result in these plugs which trap the central-mirror-cell ions, now effectively in a negative electrostatic "well" even though the central cell is also positive (but less positive than the plug-mirror cells) relative to the outside world. Any plasma ion from the central cell that climbs the magnetic gradient also approaches the large positive and repelling electrostatic potential of the plug mirror cell. Consequently, electrostatic and magnetic mirrors work in tandem to keep the plasma in the central-fusion cell.

We can further inhibit the escape of plasma by increasing the plug electron temperature, thus enhancing electron loss rates from the plug and leaving a larger "+" potential in the plugs. Or, we can increase the plasma ion density in the plugs so that there are more electrons to lose which also increases the "+" potential in the plugs. In fact, both methods were used in the Tandem Mirror Experiment[25] (TMX) at LLNL that validated the principles of electrostatic plugging.

Unfortunately, the two plug cells experienced exorbitant electron and ion loss rates in addition to high Bremsstrahlung losses due to their elevated temperature relative to the central-cell electrons. Consequently, design studies of tandem mirror commercial power reactors required large central-cell plasma volumes for the fusion process in order to make up for the externally injected energy (needed for start-up and

plasma confinement) in the end-plug cells. Power gain values, Q-values, between 5 and 10 were expected.[26]

The external plug heating power could be minimized if the plug-plasma density could be reduced and if the hot plug electrons could be prevented from exchanging energy with the relatively cool central-cell electrons. Unfortunately, neither is possible with a conventional tandem mirror. A method was needed to isolate the plug electrons from the central-cell electrons and to reduce the plasma density in the plugs.

Thermal-barrier-tandem-mirror (TBTM). An improvement came in 1979 from Baldwin and Logan,[20] also with LLNL. They proposed the "thermal barrier" concept which is a method to "thermally isolate" the hot plug electrons from the relatively cool central-cell electrons. This allowed the plasma density in the plugs to drop below that in the central cell, and yet still maintain the high "+" potential peaks in these regions required for electrostatic mirroring. The result of this is a much reduced external heating requirement for plug electrons.

Figure 2-1 is a comparison of the success in improving axial plasma confinement for the simple mirror, the conventional tandem mirror, and the thermal barrier tandem mirror (TBTM). The low ion density regions in the TBTM, Figure 2-1(C), have allowed achievement of the desired high central-cell ion density at reduced ion density in the electrostatic plugs (as compared to the conventional tandem mirror).

To characterize the thermal-barrier principle, LLNL began construction on the Mirror Fusion Test Facility[27] (MFTF-B). This experiment was designed to be the mirror-fusion equivalent of the Tokamak Fusion Test Reactor[28] (TFTR) at Princeton, New Jersey, with the ultimate goal of achieving a Q of unity, "break-even." Simultaneously, LLNL's other mirror experiment, the Tandem Mirror Experiment Upgrade[29] (TMX-U), validated the thermal-barrier concept, showing a factor of nine decrease in the central-cell loss rate over the conventional TM. A TBTM fusion reactor with a power gain 'Q' larger than 20 was now expected, but questions concerning radial plasma confinement persisted.[29]

The Mirror Fusion Test Facility (MFTF-B), or an upgrade of the TMX facility (TMX-O[30]) could have resolved or characterized these radial transport issues; unfortunately, budget constraints required elimination of MFTF-B operating funds and the smaller TMX-O never went forward. The Mirror Fusion Test Facility was completed, its magnet systems tested flawlessly (the largest superconducting system in the world), and then mothballed (1987) having never received a plasma.

Leading terrestrial designs (MARS & MINIMARS). During the construction of MFTF-B, design studies of commercial-grade thermal-barrier-tandem-mirror fusion power plants were under way. The plugging scheme for the Mirror Advanced Reactor Study[31] (MARS), completed in 1984, is shown in Figure 2-2. The acronym chosen for this study is possibly prophetic, although at the time, MARS had nothing to do with traveling to the planet Mars. While the MARS end cells provide a well-tested method of MHD stabilization, Figure 2-2 illustrates that to achieve better containment of the central-cell plasma ions, the end-plug schemes had become very complex.

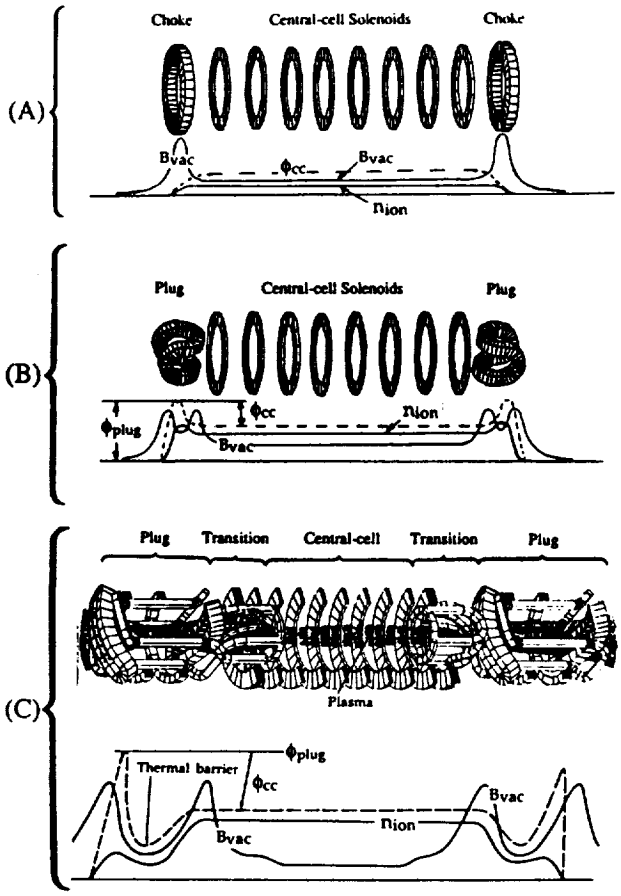

Figure 2-1. Evolution and comparison of magnetic field, electrostatic potential, and plasma-ion density in (A) the simple-mirror (SM), (B) tandem-mirror (TM), and (C) thermal-barrier-tandem-mirror (TBTM).

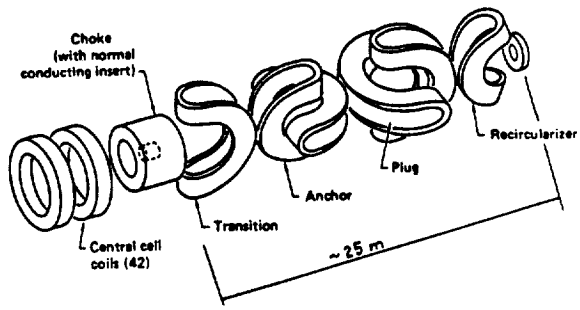

Figure 2-2. Mirror Advanced Reactor Study[31] (MARS); a complex end plug configuration.

MINIMARS. In 1984, a simplified plugging scheme was identified and studied at LLNL.[32] A new commercial reactor design study based on this plugging scheme was completed in 1986 called MINIMARS for MINI-Mirror Advanced Reactor Study,[33] Figure 2-3.

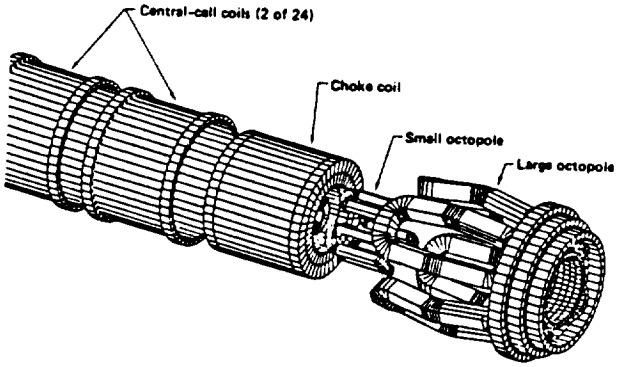

Figure 2-3. MINIMARS[33]; a simpler end plug.

The resulting short, compact end cells enable ignition to be achieved with much shorter central-cell lengths, considerably improving the economy-of-scale characteristics for small (250-600 MWe) reactors. In particular, MINIMARS achieves a larger Q than MARS in a reactor of half the power. MINIMARS is designed to have a power gain of Q=32 for a relatively small 600 MWe power plant. This high power gain underscores two advantages of linear open magnetic confinement systems over toroidal closed magnetic confinement systems: (1) the efficient use of the linear magnetic field (~10 times greater than in closed systems) and (2) the ability to use direct energy conversion of the plasma charged-particle energy, thereby improving the overall plant efficiency to above 50%.

Application of design principles to the TBTM

All fusion-grade plasmas emit the four radiations previously described and shown in Figure 1-7. In all cases, there will be a substantial amount of waste power radiated from the plasma. For a 4-GWt fusion power plant in space, as much as 50%, 2 GW, of waste radiation must be released to space, somehow. If we look at the MINIMARS design, Figure 2-3, we see that the plasma, at ~300 million kelvins, is surrounded by metallic superconducting coils at 4.2 kelvins. On earth, this represents a serious thermal management problem; in space, it represents an un-manageable problem. MINIMARS is a TBTM solution that is unsuitable for space propulsion.

DP-1: Provide maximum direct access to space for waste radiation. We seek to apply the first design principle to find ways to provide direct access to space for as much of the waste radiation as possible. In searching the literature, we found that at the end of the MINIMARS design study, a new, better method of central-cell plasma stabilization was identified and studied, consisting of a ripple-magnetic field and an electrically-conducting wall (in contrast, MINIMARS relied on a smooth central-cell magnetic field for stability). In this new stabilization method, discrete circular coils are used rather than the pancake coils used in MINMARS. These coils are placed along the length of the central cell, with inter-coil distances that form magnetic-field ripples of 10-15%, being defined by:

$$B_{(ripple)} = \frac{B_{MAX} - B_{MIN}}{B_{AVE}} = 2 \cdot \frac{B_{MAX} - B_{MIN}}{B_{MAX} + B_{MIN}} \qquad (2.3)$$

An example of magnetic-field ripple is pictured in Figure 2-4, with the ripple matched to the corresponding superconducting current elements. The spacing between the coils provides an exit path for waste radiation and radiated thermal heat to escape to deep space.

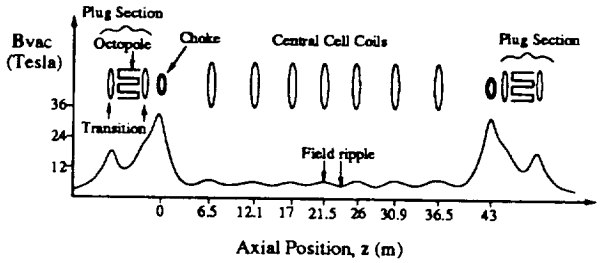

Figure 2-4. Magnetic field ripple.

There are other structures that surround the plasma in addition to the superconducting coils, the most important being the electrically-conducting wall that completely encircles the plasma, needed for plasma stability purposes. Applying the design principle to this structure leads us to seek construction materials that are semi-invisible to the plasma-generated neutron and x-ray radiation. We propose that it is possible to construct the electrically-conducting wall from three materials, molybdenum, graphite, and advanced carbon fiber, such that between 50-70% of the Bremsstrahlung and neutron radiation generated in the plasma pass through this structure.

Consequently, applying this first design principle to the TBTM configuration has led us to a space-propulsion-based engineering-design solution that we call the Mirror Fusion Propulsion System[11] (MFPS), shown in Figure 2-8.

In MFPS, the discrete superconducting coils are called Shield-Coil Units (SCUs) and the electrically-conducting wall is called the Radiator-Reflector Unit (RRU). The SCUs produce the magnetic field that contains the radial pressure of the reacting d-^{3}He and other fusion reaction particles in the Central-Mirror Cell (CMC). The RRU is one key component of the Central-Mirror Cell, consisting of a thin-walled rippled

tube that surrounds the plasma. The RRU wall is composed of three layers: (1) the inner layer is a thin foil of molybdenum 10-50 μm thick, (2) the middle layer is graphite, about 1 cm thick, and (3) the third layer is carbon fiber, also about 1 cm thick. The RRU performs four functions: (1) the molybdenum layer reflects synchrotron radiation back into the plasma where it is absorbed, thereby increasing the power available for thrust; (2) the graphite layer (in proximity to the plasma surface) aids stabilization of the plasma by acting as an electrically conducting wall, producing an image-current counter force to growing plasma instabilities; (3) the carbon fiber layer acts as a "blackbody" radiator, thereby minimizing external cooling-system mass and providing directional structural strength; and (4) the three layers together allow most of the neutrons and over half of the plasma x-rays (Bremsstrahlung) to pass directly through the RRU into deep space (see Figures 2-5 and 2-6) thereby reducing the RRU temperature.

DP-2: Operate components as passive radiators to minimize cooling-system mass. In addition to neutron and x-ray radiation, the RRU also absorbs a small amount of plasma, synchrotron radiation, and radiated thermal heat from the Shield-Coil Units (SCUs). The single heat-sink term is provided by the carbon fiber surface acting as a "blackbody" radiator, with most of the radiated heat going directly into space (Figure 2-5).

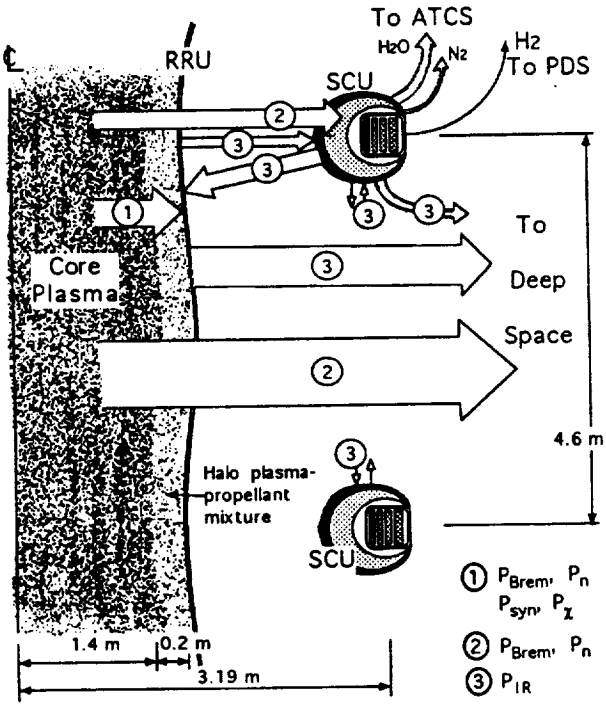

Figure 2-5. Waste power flow in MFPS.

The strategy used to minimize heat absorption in the RRU (wall thinness and low cross-section for radiation) cannot be used with the SCUs, because they are inherently thick, and materials with large interaction cross-sections are desired. Consequently, the surfaces of the SCUs are also operated as "blackbody" radiators because they intercept a fraction (~24%) of the outgoing waste radiation (Figure 2-5).

DP-3: Optimize the plasma fuel, fuel mix, and temperature for best specific jet power. There is a plasma-operating window with relatively good percent-power-available for thrust (Figure 1-6). Where we desire to operate in this regime is determined by other, more subtle criteria that include component temperatures; e.g., Figure 2-6 illustrates the advantage gained in optimizing the fuel mix (minimizing waste heat) and providing direct access to space for the radiation (minimizing heat absorption in the engine).

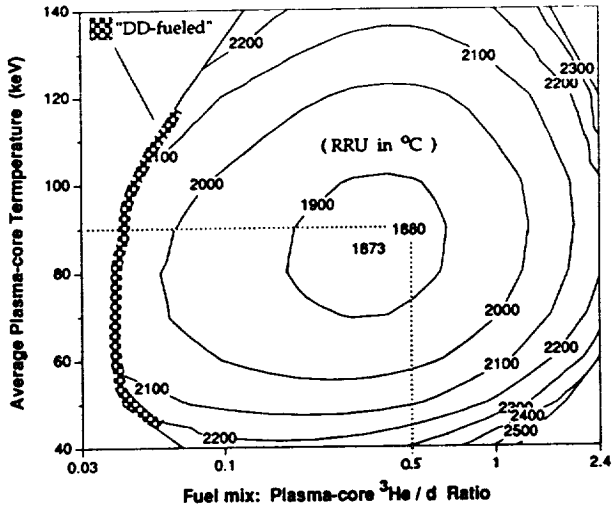

Figure 2-6. RRU temperature in a 4-GWt MFPS versus the plasma temperature and fuel mix.

Incorporating fuel-mix optimization and direct access to space for waste heat minimizes component temperatures while allowing the highest possible power operating levels. Operating components as blackbody radiators reduces external cooling-system mass, further improving specific jet power. There are numerous other factors that will determine the exact plasma-core fuel-mix and temperature optimization, and these include the fraction of ^{3}He burn up (acquisition and cost problem), the magnetic field strength and associated structural masses, the radiator masses, the shielding materials and masses, the specific jet power and overall IMLEO, and more. Of these, the specific jet power is one of the most important and Figure 2-7 shows that the desired fuel mix moves towards a one-to-one ^{3}He-to-d ratio.

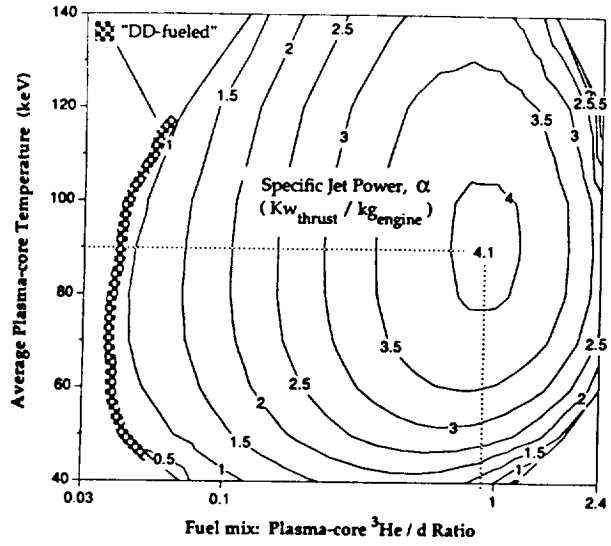

Figure 2-7. Specific jet power in a 4-GWt MFPS versus the plasma temperature and fuel mix.

Space-based TBTM design: MFPS Subsystems Overview. The generic MFPS is about 79 m long and 8 m in diameter and produces 4-GWt of fusion power. Figure 2-8 shows MFPS and nine of its major components or subsystems.

Central Mirror Cell (CMC). The function of the CMC is to contain the plasma core in a stable, ignited mode. The CMC consists of six components or subassemblies: (1) the Reflector-Radiator Unit (RRU), (2) seven Shield-Coil Units (SCUs), (3) two Choke Coil Units (CCUs), (4) a Fuel Pellet Injection Assembly (FPIA), (5) a Propellant Injection Assembly (PIA), and (6) a High-Compression Structure (HCS).

Forward and Aft Mirror Cells (FMC and AMC). The FMC and AMC, located forward (crew side) and aft (propellant-exhaust side) of the CMC, respectively, each consist of one large octopole magnet and several shaping magnets that aid central-cell plasma stability during startup and axial plasma confinement during all operations.

Direct Converter Assembly (DCA). The DCA, located forward of the FMC, directly converts charged-particle kinetic energy to electricity. The electrical power is used for space vehicle electrical loads and recirculation power for fusion reactor subsystems.

Power Conditioning Subsystem (PCS). The PCS consists of several subsystems responsible for the distribution of power from the DCA to the reactor and ship systems. It also provides the charging power for the MFPS Reactor Ignition Subsystem used to restart the fusion reactor and for pellet injection.

Propellant Delivery Subsystem (PDS). The PDS is responsible for pumping the liquid-hydrogen propellant through the superconducting coils to provide cooling of the coils. The PDS then injects the heated propellant into the central-cell plasma through its Propellant Injection Assembly (PIA) located on the CMC.

Exhaust Neutralizer Assembly (ENA). The ENA neutralizes the plasma/propellant mixture, thereby detaching the particles from the magnetic field lines to produce thrust. The ENA contains neutral gas-injection jets for charge exchange with the hot plasma/propellant exhaust.

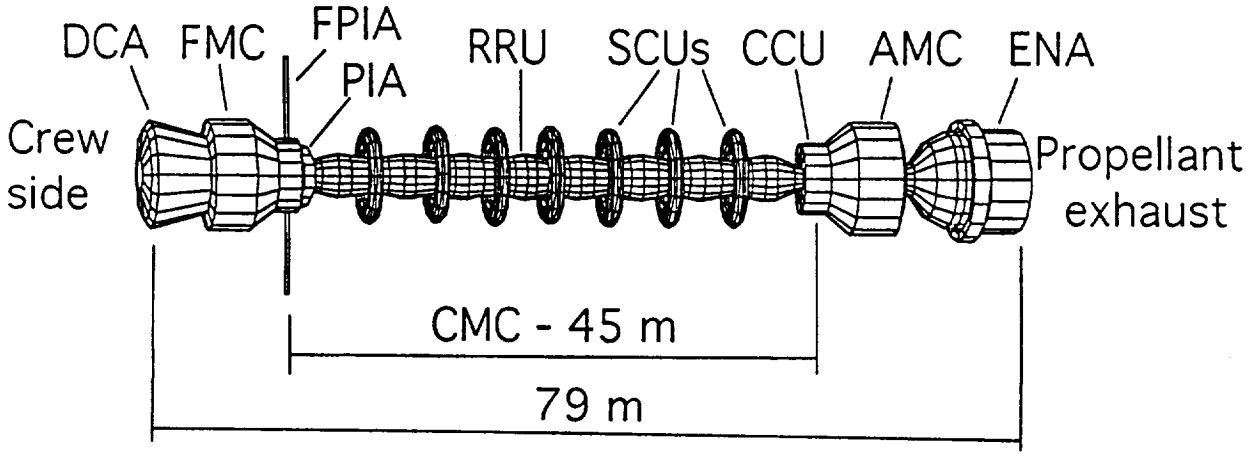

ATCS	Active Thermal Control Subsystem (not shown)
DCA	Direct Converter Assembly
FMC	Forward Mirror Cell
CMC	Central Mirror Cell
FPIA	Fuel Pellet Injection Assembly
PIA	Propellant Injection Assembly
RRU	Reflector-Radiator Unit
SCU	Shield-Coil Unit
CCU	Choke Coil Unit
AMC	Aft Mirror Cell
ENA	Exhaust Neutralizer Assembly
HCS	High-Compression Structure (not shown)

Figure 2-8. The Mirror Fusion Propulsion System (MFPS) - drawn to scale.

Active Thermal Control Subsystem (ATCS). The ATCS consists of radiator panels and pump assemblies forward of the direct converter, and pipes distributing the cooling fluids to all shield/magnet assemblies throughout the mirror cells. The ATCS has two subsystems: (1) the H_2O Subsystem and (2) the N_2 Subsystem.

(2) Field-Reversed-Mirror (FRM) Configuration

In this paper, we use the FRM[34] and field-reversed-configuration (FRC) terminology rather loosely. The FRM is a little more specific in that it refers to an FRC which is formed and then held in place by a magnetic mirror, usually a simple mirror (SM). Historically, the FRM came to identify magnetic-field reversal as initiated by neutral beams (Figure 2-9), whereas the FRC came to identify magnetic-field reversal as initiated by a reversed-field theta-pinch device (Figure 2-10). For the most part, FRC and FRM can be used interchangeably.

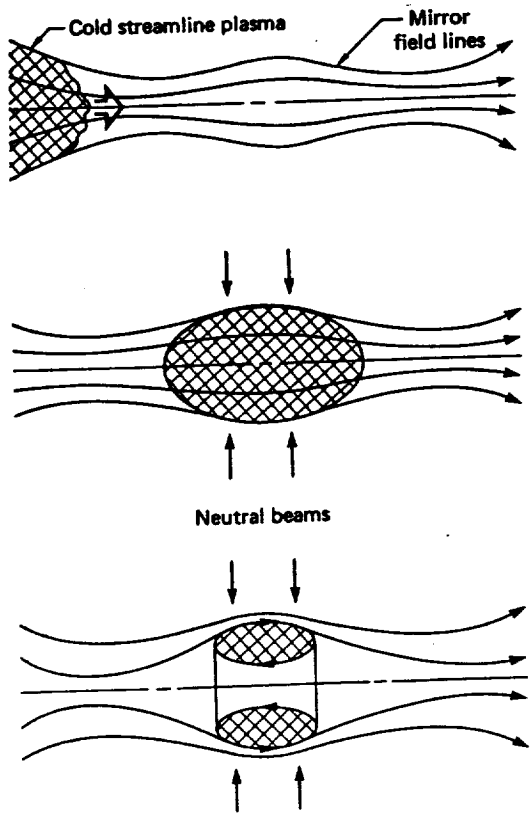

Figure 2-9. FRM formation using neutral beams.[34] In the top diagram, a target plasma is injected into a magnetic-mirror field. In the middle diagram, neutral beams heat and build up the target plasma to field reversal. In the bottom diagram, neutral beams sustain the reversal state and fuel the plasma.

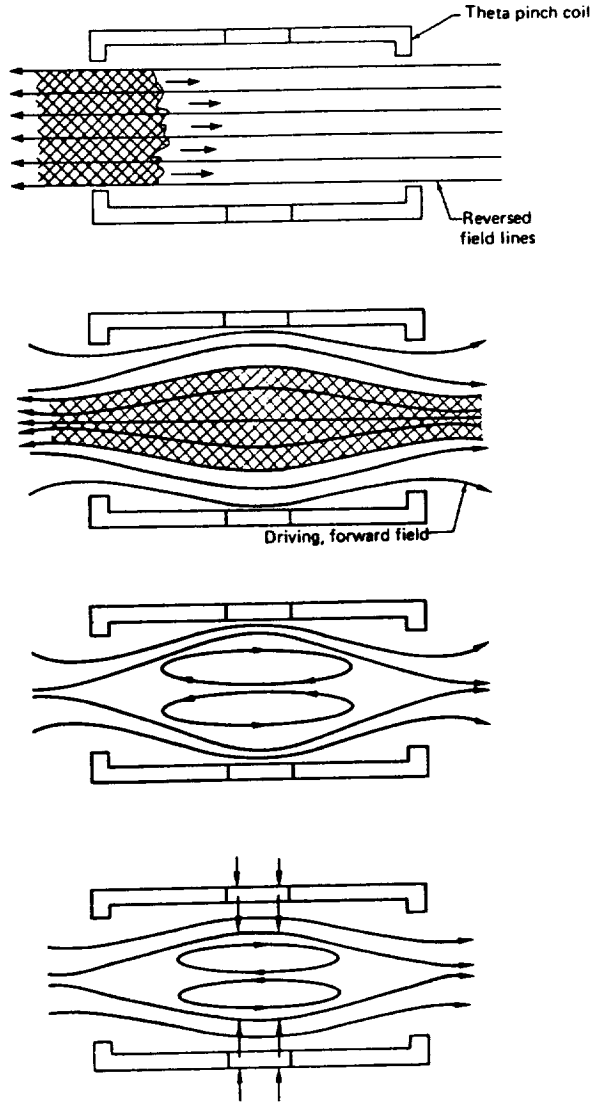

Figure 2-10. FRC formation using the reversed-field theta-pinch (RFTP) approach.[34] In the top diagram, a cold plasma is injected through a theta-pinch coil along a reversed-biased magnetic field. In the second diagram, the theta-pinch coil is pulsed to produce an oppositely directed compressional B-field. In the second-from-the-bottom diagram, the plasma column with reversed central magnetic flux tears at the ends, magnetic lines reconnect, and reversed-field confinement is firm. In the bottom diagram, the plasma is sustained by neutral beams and heated by beams or magnetic compression.

The FRM and FRC's have very high plasma betas, averaged over the separation volume, ranging from 0.5 to 1. The plasma beta is a measure of the system's magnetic field efficiency at containing the plasma and is defined as:

$$\langle\beta\rangle = \frac{\text{plasma kinetic pressure}}{\text{magnetic field pressure}} \qquad (2.4)$$

A high plasma beta is a very desirable feature; for comparison, MFPS's is very desirable at 0.7 but the Tokamak's is poor at only 0.05-0.20.

A field-reversed configuration (FRC) is an elongated compact toroid that ideally contains no toroidal field (Figure 2-11). Simply said, an FRC is a ring of current in a magnetic field. The edge layer results in a natural divertor that deposits exhaust plasma for thrust or direct energy conversion for electricity. Unfortunately, the FRM/FRCs have not been as thoroughly investigated as the TBTM. Nevertheless, key issues have been identified and are being assessed.

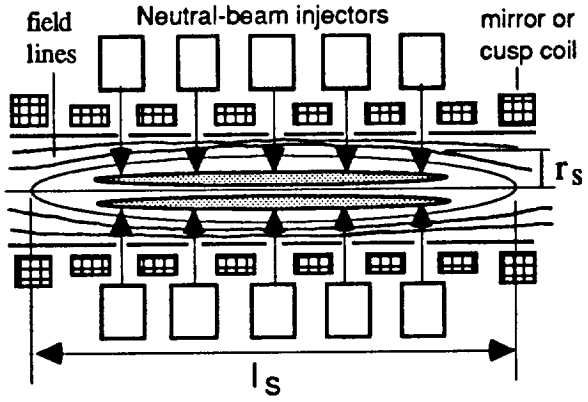

Figure 2-11. Burn-section of an FRC. r_S is the separation radius and l_S is the separation length.

"s" is an important FRM/FRC parameter which is defined as the number of internal ion gyroradii between the field null and the separation radius, r_S. "s" is a good measure of the field-reversed plasma's "closeness" to destabilizing or stabilizing effects. On axis is a field null, zero magnetic field, and ion-orbits passing through this region are relatively large which has a stabilizing effect on the plasma as a whole. So far, small s-value FRCs (s<3) are robustly stable. But this makes for a very small plasma volume and a low power reactor (~20-200 MWt/cell).

It is expected that earth-based power plants will require s-values of around 20. The Large-s Experiment[35] (LSX) produced s-values equal to 4 by the field-reversed theta-pinch method of FRC formation. It is presently believed that s-values up to 20 or more may be achieved by using the field-reversed theta-pinch method to bring s up to 3, translate the FRC to the burn section (Figure 2-11), and then sustain and build-up the FRC to s=20 using neutral beams.

Application of design principles to the FRM

This Section is highly speculative because the understanding of the FRM/FRCs is not at the same level as that of the magnetic mirror machines although other studies have suggested using the FRC for space propulsion.[38]

DP-1: Provide maximum direct access to space for waste radiation. Presumably, we desire to do to the FRC the same as we did with the TBTM, namely, space the magnetic coils widely to provide large exit paths for plasma radiation. In fact, because of the field-reversal self-containment, it should be possible to open wide gaps between the coils as in the hypothetical space-based design shown in Figure 2-12. Unfortunately, there are other components that will interfere with exiting radiation, e.g., the neutral beam injectors. Presumably, the conducting-wall could be treated as in MFPS.

DP-2: Operate components as passive radiators to minimize cooling-system mass. Most of the components can be treated in the same manner as MFPS, however the neutral beam injectors will probably require some form of active cooling.

DP-3: Optimize the plasma fuel, fuel mix, and temperature for best specific jet power. We have not performed a detailed optimization due to the speculative nature as to the final design solution of a successful FRC.

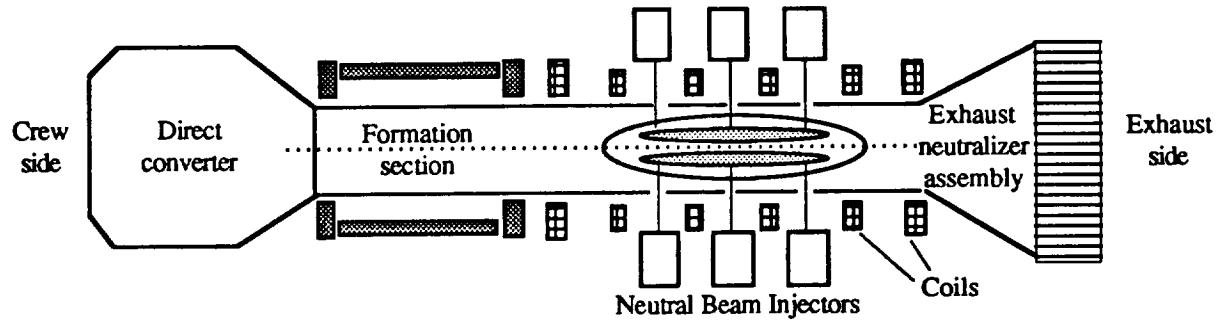

Figure 2-12. A Hypothetical Space-Propulsion-Based FRC.

The FRCs are potentially very stable, efficient, and simple. However, by their very nature, they produce relatively low-volume (thin-ring) plasmas. As a consequence, the unit mass-to-power ratio may not be favorable. The FRCs warrant further study, particularly as efficient, utility-based fusion power reactors.

(3) Levitated-Dipole-Field[39] (LDF) Configuration

A hypothetical space-based LDF fusion reactor is shown in Figure 2-13. It is necessarily large and one can easily imagine the associated large masses involved with a complete engine. In a previous space-propulsion-based LDF design study,[37] the levitated ring alone had a mass of 1180 Mg.

Basic operation. In principle, the superconducting levitated ring is charged with about 40-50 MA of current, and then levitated between the three positioning coils. A gas is introduced, and RF energy or neutral beams ionize it. It quickly becomes trapped on the levitated dipole's field. Neutral beams are used to heat and build up the near-coil plasma until the adequate temperature and density exist for fusion to occur. Although diffusion down the dipole field is much greater than up it, the hot fusion-grade plasma hugs the ring (Figure 2-14). Far away from the ring, the plasma should be a desirable, relatively cool, 10-100 eV. In the previous study,[37] the surface temperature of the ring was expected to be about 2700 K, in steady-state. Neutron power that penetrates into the ring is removed by internal refrigeration units that pump heat to the ring surface.

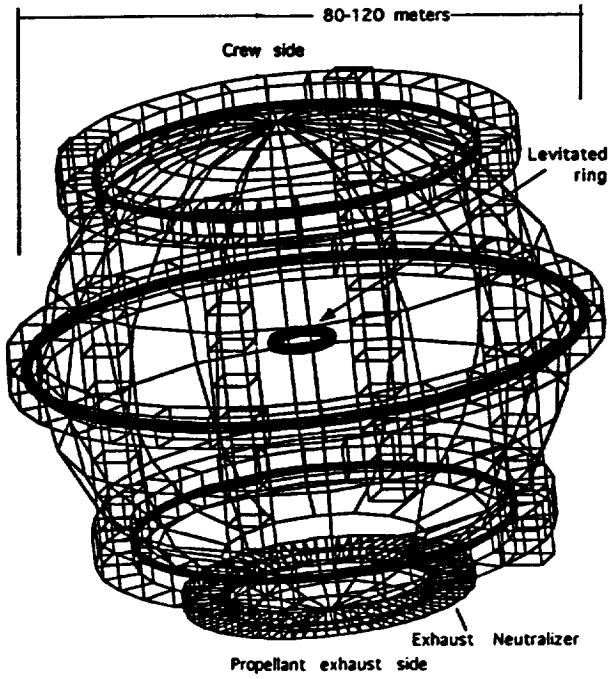

Figure 2-13. Hypothetical space-propulsion-based LDF configuration.

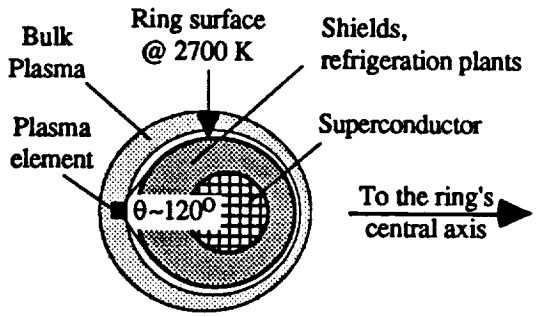

Figure 2-14. Close up view of the superconducting levitated ring/plasma region.

Application of design principles to the LDF

DP-1: Provide maximum direct access to space for waste radiation. In this scenario it is desirable to push the plasma away from the coil. Looking closely at Figure 2-14, you will notice that there is more plasma on one side than on the other. That is because the magnetic filed is stronger in the middle of the ring, and magnetic mirroring is occurring somewhat analogous to the Earth's dipole-field-mirroring of trapped charged particles. The idea now is to increase the magnetic field strength further, by increasing the ring current, thereby forcing the bulk of the fusion-grade plasma a little distance away from the ring, perhaps only one-half of a meter. Figure 2-15 shows that even one-half of a meter makes a significant difference. Now much less than 50% of the neutrons and Bremsstrahlung radiation is falling on the ring, which means its surface temperature will drop and so will its shielding and internal refrigeration requirements. In fact, this has recently been proposed.[39]

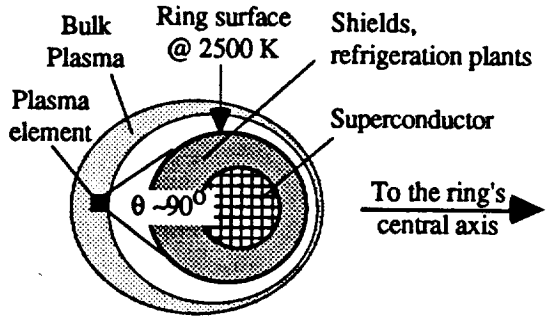

Figure 2-15. Close up view of a high-field superconducting ring/plasma region.

DP-2: Operate components as passive radiators to minimize cooling-system mass. The LDF reactor concept is already the ultimate in application of this principle.

DP-3: Optimize the plasma fuel, fuel mix, and temperature for best specific jet power. This analysis has not been carried out in detail, however, we note that it is probably better to operate the d-^{3}He plasma rich in ^{3}He to minimize production of the deeply penetrating high-energy neutrons. This might reduce the shielding and internal refrigeration plant masses. These ideas have already been proposed.[37]

A major problem with pushing the plasma away from the ring, via a steeper magnetic field gradient and more mirroring action, is that the entire magnetic field is being produced by a single coil. A 12-meter diameter coil with 50 MA of current (1-meter square cross section) produces an extremely high magnetic field at the coil's surface, in the 10's of Tesla. If the coil cross-section expands, to reduce the internal field, then the shielding masses skyrocket due to the geometry of expanding concentric volumes. Nevertheless, there are very few superconducting materials, developed or identified, that can remain superconducting at such high magnetic fields.

For the remainder of this paper, we shall focus on the ability of the Mirror Fusion Propulsion System to complete human- and robot-piloted space missions.

Part 3
Space Mission Scenarios

In this part we define specific mission scenarios relevant to the fusion propulsion regime. These mission scenarios include (1) a 90-90-90-day human-piloted Mars-exploration mission with continuous mission-abort capability, (2) a human-piloted Saturn-exploration mission with continuous mission-abort capability, and (3) a post-design-life robot-piloted mission to the large gravitational focal zone of the Sun called the solar-gravity-lens (SGL) mission.[44] The trajectories are modeled similar to those of other studies[40,41,42,43]. These missions can be accomplished with less propellant mass and with shorter flight times using the Mirror Fusion Propulsion System (MFPS) than is possible with other proposed propulsion systems due to (1) MFPS's ability to provide steady, continuous thrust at a magnitude of up to 2 cm/sec^2, and (2) MFPS's high specific impulse (Isp) that can be varied between 37,000 seconds (human-piloted Mars mission) and ~350,000 seconds (post-design-life robot-piloted-MFPS SGL mission).

The method of patched conics was used for the orbital transfers with assumptions made to simplify the analysis. The results are applicable to preliminary studies of these missions. The assumptions are:

a) the planet orbits are coplanar and circular,
b) the orbital velocities of the planets are constant,
c) parking orbits at the planets of interest are circular,
d) the gravitational effects of all bodies except the Earth, Sun, and target planet are neglected, and
e) the gravitational attraction of the Earth, Sun, and target planet are treated as point sources.

Mars human-piloted mission

Chemical propulsion systems are limited to a specific impulse of 450-to-500 seconds. Solid-core Nuclear Thermal Rockets are limited to a specific impulse of about 1,000 seconds. Proposed human-piloted missions to Mars using these propulsion technologies result in initial propellant loads of 600-to-1,500 tonnes and flight times of 7-to-9 months.

Due to the MFPS's high exhaust-jet power (2 GW) and its specific impulse of 37,000 seconds, MFPS can achieve an acceleration of about 1 cm/sec^2 at a propellant flow rate of only 30 grams/second. This is the desirable operating regime for MFPS human-piloted missions to Mars.

Figure 3-1 shows the IMLEO of MFPS and NTR-gas core propulsion systems versus mission window for constant 90-day travel times to or from Mars.

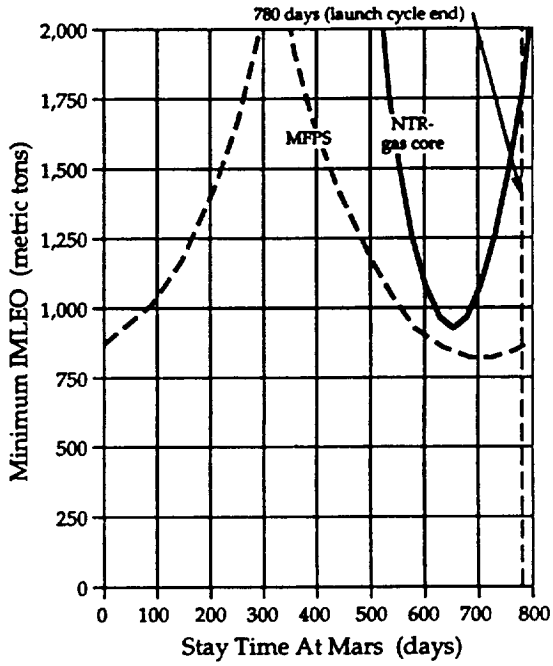

Figure 3-1. IMLEO for constant 90-day travel times to and from Mars.

Comparing MFPS to other propulsion systems which cannot compete in the 90-day Mars travel time regime, Figure 3-2 plots the IMLEO versus one-way flight times to or from Mars. Because MFPS has the capability of completing eight 90-90-90-day Mars-type missions, its actual engine IMLEO should be 520,000 / 8 = 65,000 kg.

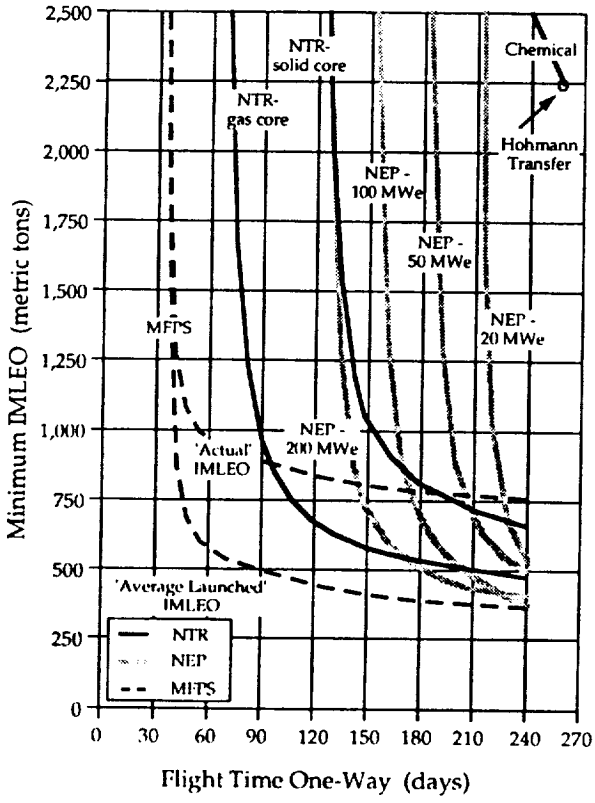

Figure 3-2. IMLEO for various propulsion systems versus travel time to or from Mars.

Outer solar system enabler. The MFPS is capable of supporting human-piloted missions to the outer solar system, beyond Mars, which are simply not within the reach of chemical or nuclear thermal propulsion systems. Figures 3-3, 3-4, 3-5, and 3-6 show certain performance characteristics of MFPS.

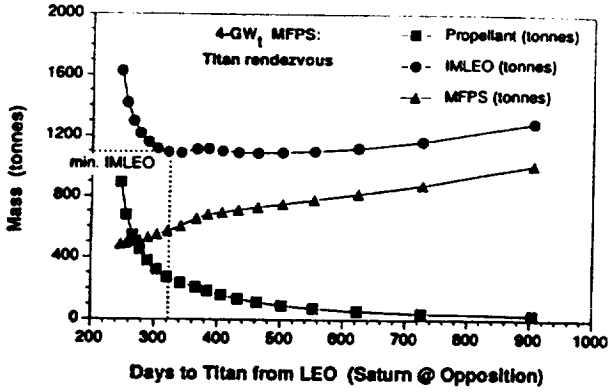

Figure 3-3. Days to Titan from LEO versus Mass.

The minimum IMLEO is a trade-off primarily between coolant/propellant flow rate through the superconductor and the associated shielding mass necessary to limit the neutron-power deposited in the superconductor.

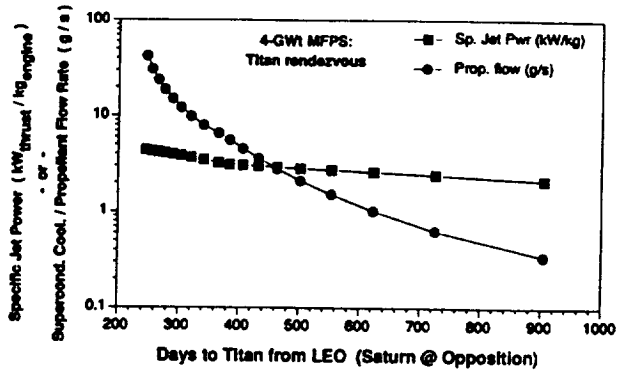

Figure 3-4. Days to Titan from LEO versus Specific Jet Power.

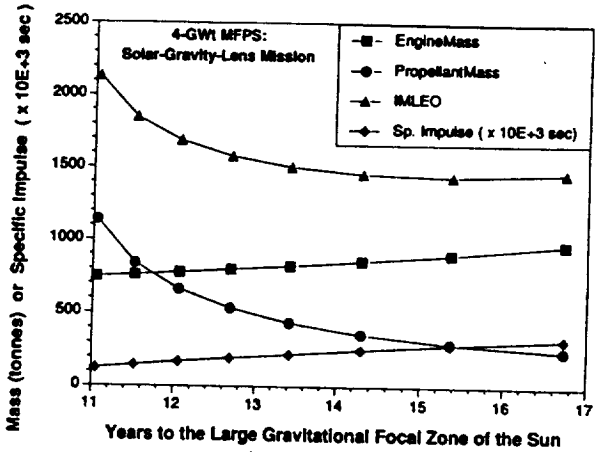

Figure 3-5. Years to the Large Gravitational Focal Zone of the Sun (~500 A.U.) versus Mass and Specific Impulse.

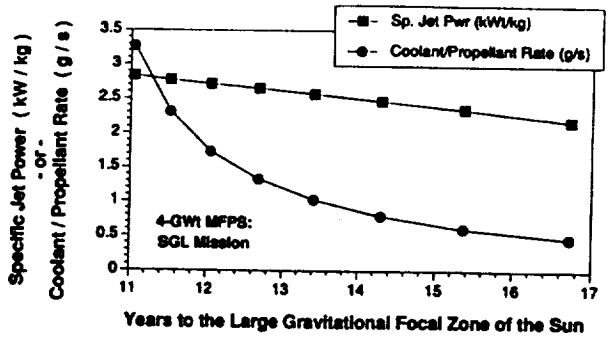

Figure 3-6. Years to the Large Gravitational Focal Zone of the Sun (~500 A.U.) versus Specific Jet Power.

Part 4
Scenario for a Research and Development Program

To accomplish colonization of our solar system, fusion propulsion offers an attractive mission enabling approach. With a background of many years of research and development activities in the terrestrial program, confinement concepts which can be applied toward a process that could lead to a fusion space powered propulsion system are available. Further, the technical aspects of space travel point one in a different direction from the terrestrial application where inert mass carries less penalty than space. The proof is not expected to be quick; and, hence, this is an appropriate time to perform critical technology developmental experiments. A properly structured program is one intended to demonstrate basic confinement principles. The program should perform such experimental verifications in a time-frame whereby fusion would be available in the future, coincident with reaching a commitment to a wider exploration of space. As such a program is formulated, it must be designed such that the space fusion propulsion systems provide inherent design features which avoid the limitations of chemical and nuclear fission systems.

The managerial extremes in the structuring of an initial space fusion propulsion developmental program range from simply the conduct of analytical studies as a minimal effort, to the other extreme using the most optimistic approach of proceeding directly with a best estimate design toward a full-scale extrapolation of confinement schemes. We opt for a middle ground, one in which first principles are established, but then which proceeds at an accelerated pace to a net power design.

The rationale for the selection of a middle ground is based upon experience with the implementation of developmental technology programs and upon the importance of fusion to space. Studies, although cheap, are not the proper means to produce results. In the case of space fusion where data are needed, studies tend to delay obtaining critical experimental information. The other extreme, proceeding directly to full scale design experiments at the onset, is not considered a good economical choice, and not necessarily a rapid means to obtain answers. Full scale experiments where net power is produced are necessary and should be attained at an accelerated pace, one where we would proceed without a full characterization of the reactor's physics.

We simplify and leverage the program start process by employing past experiences as our departure point. First, the key issues are considered, and then those issues are prioritized.

The next question is how should one proceed toward the selection of one or alternate confinement concepts. The conduct of a workshop which exposes all potential concepts to a peer review process is a sound means to get designs and issues out on the table for evaluation. As one output from the workshop, a better definition of design opportunities for reactor related research will be identified. For example, it is easy to anticipate that any investment in high temperature superconductor and reduced mass cooling systems will provide significant benefits to the space fusion program. For space, clearly one top level priority is plasma confinement. Next is system mass.

One objective in the early program phases is to continue to refine the program costs associated with the development of a practical space propulsion system. Balanced with program expenses we take cost credits for the positive additional benefits to humankind that are expected to result from common-use derived technologies which will be given birth from the program. High temperature superconductors fall into that category.

What we consider to be the next step, is to become convinced that any selected confinement concept has technical validity. That means we require the demonstration of proof-of-principles. At the current developmental phase in fusion, from a program management perspective, we consider the conduct of applied research on at least two configurations to be an essential feature. In the establishment of any rating criteria, minimal reactor mass is the most important parameter once plasma burning and other operational conditions have been satisfied. System considerations have the major driving influence on space operated vehicles. Consequently, by minimal mass we refer to the total propulsion system mass, not simply the reactor mass. This initial program activity is depicted below.

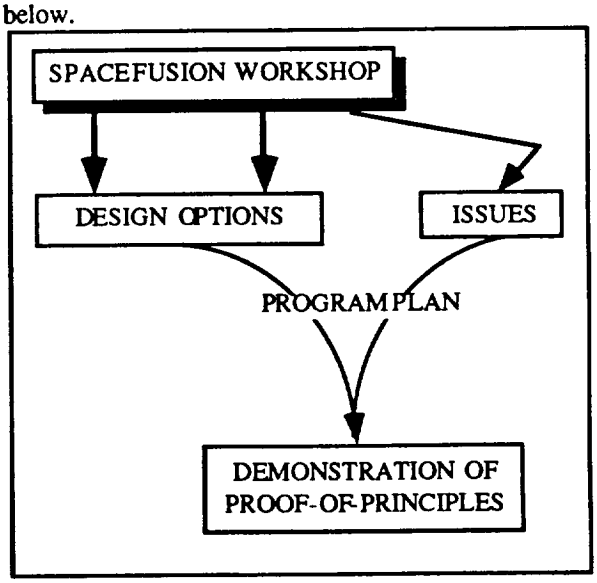

The program plan for each of the two concepts is expected to present the major issues to address, and the program approach for resolution of issues will be identified. Key milestones are identified for criteria as guides to continue along particular investigative paths or whether options are to be pursued. The current state

of fusion technology permits such judgments to be made without undue risk. Once proof-of-principle experiments have been demonstrated, the plan should be to progress rapidly to full scale net power demonstrations as presented below.

We recognize that this approach may lead to retracing some steps, if technical obstacles are encountered. We dub this an "accelerated" approach. The risk is considered to be worthwhile in view of the potential gain.

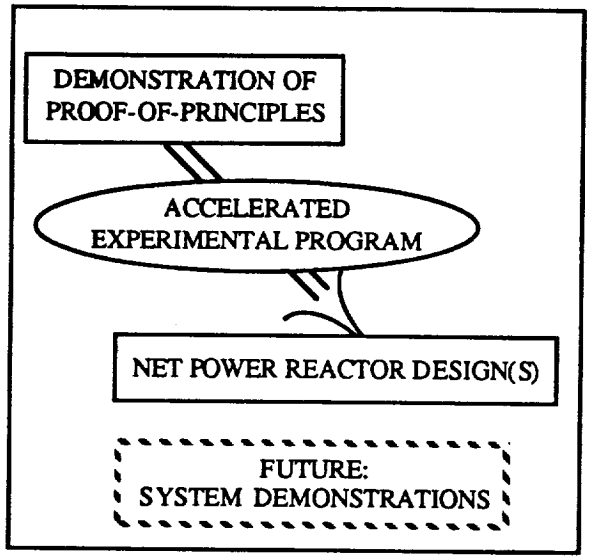

By the rapid transition to full scale reactors, program costs can be minimized. Risk is reduced by making maximum use of existing analytical capabilities either already developed or developed in the proof-of-principle experiments. Confidence that the program is on the proper track is gained following the demonstration. Full understanding and characterization of reactor physics is not initially accomplished but is deferred. The need to modify the initial design in order to meet the large variety of applications is expected to follow. That is considered typical of the introduction of new technologies. For example, combustion instabilities were not performed by Dr. Goddard in the process of the development chemical propulsion prior to developing and flying full scale launch vehicles.

In this program scenario we are concerned basically with demonstrating the physics of confinement for reactors having the capability for use as high power space propulsion systems. Great reliance is placed upon open forum discussions using a good peer review process. Demonstration of confinement is the first program priority. To be employed in a flight vehicle there are many other important considerations, such as system safety, reliability, economics, and performance, all of which are interrelated. These topics are treated in greater depth in "Fusion Energy for Space missions in the 21st Century," NASA TM 4298.

Acknowledgments

The authors wish to acknowledge the following people and their contributions to this paper. We thank Dr. Heino Nitsche (LBL) for his encouragement and usual selfless support. We thank Dr. Kathleen Brennan for performing many endless hours of computer-program optimization runs. We thank Dr. Daniel R. Dietderich (LBL) for his comments on application of high-Tc, high-field superconductors to MFPS and on prospects for their development. And we thank Dr. Giovanni Vulpetti for discussions concerning the INTERFLIGHT[45] and the solar-gravity-lens mission.

References

1. Miller, T. J., Clark, J. S., a nd , J. W.; Nuclear Propulsion Project Workshop Summary, in Space Nuclear Power Systems; Eighth Symposium, Part 2; El-Genk, M. S. and Hoover, M. D. Eds.; Albuquerque, NM, (1991) 84.
2. Clark, John S.; A Comparison of Nuclear Thermal Propulsion Concepts: Results of a workshop, in Space Nuclear Power Systems; Eighth Symposium, Part 2; El-Genk, M. S. and Hoover, M. D. Eds.; Albuquerque, NM, (1991) 740.
3. International Fusion Research Council; Status Report on Controlled Thermonuclear Fusion, in Nucl. Fusion **30** (1990) 1641.
4. Englert, G. W.; "Toward Thermonuclear Rocket Propulsion," New Scientist **16**, #307, 16 (1962).
5. Wittenberg, L. J.; Cameron, E. N.; Kulcinski, G. L.; Ott, S. H.; Santarius, J. F.; Sviatoslavsky, G. I.; Sviatoslavsky, I. N.; and Thompson, H.E.; A Review of ^{3}He Resources and Acquisition for Use as Fusion Fuel; Fusion Technology, **21**, July 1992.
6. Kulcinski, G. L. and Schmitt, H. H.; Fusion Power from Lunar Resources; Fusion Technology, **21**, July 1992.
7. Emmert, G. A., El-Guebaly, L., et al.; Possibilities for Breakeven and Ignition of D-^{3}He Fusion Fuel in a Near Term Tokamak; Nuclear Fusion, Vol. 29, No. 9 (1989).
8. McNally, J. R. Jr., Physics of Fusion Fuel Cycles; Nuclear Technology/Fusion, Vol. 2 (1982).
9. McNally, J. R. Jr.; Fusion Reactivity Graphs and Tables for Charged Particle Reactions; ORNL/TM-6914 (1979).
10. Howerton, R. J., UCRL-50400, Vol. 21, Pt. A; LLNL (1979).
11. Carpenter, S.A. and Deveny, M.E.; Mirror Fusion Propulsion System (MFPS): An Option for the Space Exploration Initiative (SEI); Paper No. IAF-92-0613 presented at the 43rd Congress of the International Astronautical Federation, August 28-September 5, 1992, Washington, DC.
12. Hawke, R. S.; Devices for Launching 0.1-g Projectiles to 150 km/s or More to Initiate Fusion, Part 2, Railgun Accelerators; UCRL-52778 Part 2, LLNL, 1979.
13. Hawke, R. S.; Fusion Fuel Pellet Injection with a Railgun; J. Vac. Sci. Technol. A 1 (2), Apr.-June 1983.

14. McCool, S. C., Edmonds, P. H., and Castle, G. G.; An Assessment of the Feasibility of Fueling a Tokamak Reactor with Lithium Titride Pellets; Fusion Technology, Vol. 21, 1992.
15. Wittenberg, L. J.; Helium-3 Fueling Concepts for Magnetically Confined Fusion; 12th Symposium on Fusion Engineering, (1987) IEEE Cat. No. CH2507-2/87/0000-0787.
16. Post, R.F.; Special Review Paper, The Magnetic Mirror Approach to Fusion; Nucl. Fusion 27, No. 10 (1987).
17. Post, R.F.; a paper presented at the "Classified Conference on Thermonuclear Reactors held at Denver on June 28, 1952," U.S. Atomic Energy Commission, Technical Information Service, Oak Ridge, Tenn., Report No. WASH-115, December, 1952.
18. Dimov, G. I., Zakaidakov, V. V., and Kishinevskii, M. E. (1976). *Fiz. Plasmy* **2**, 597 [*English transl.: Sov. J. Plasma Phys.* **2**, 326-333].
19. Fowler, T. K., and Logan, B. G. (1977). *Comments Plasma Phys. Controlled Fusion Res.* 2, 167-172.
20. Baldwin, D. E., and Logan, B. G. (1979), Phys. Rev. Lett. **43**, 1318-1321.
21. Cristofilos, N.C.; Trapping and Lifetime of Charged Particles in the Geomagnetic Field; UCRL-5407, November 28, 1958.
22. Post, R. F. and Santarius, J. F.; Open Confinement Systems and the D-^{3}He Reaction; Fusion Technology, **22**, August 1992.
23. Santarius, J. F.; Magnetic Fusion for Space Propulsion; Fusion Technology, **21**, May 1992.
24. Moir, R. W., and Post, R. F. (1969), *Nucl. Fusion* **9**, 253-258.
25. TMX Group; Summary of Results from the Tandem Mirror Experiment (TMX); UCRL-53120, February 26, 1981.
26. Moir, R.W., et al.; Preliminary Design Study of the Tandem Mirror Reactor (TMR); UCRL-52302, Lawrence Livermore National Laboratory (LLNL), July 15, 1977.
27. Baldwin, D. E., Logan, B. G., et al.; Physics Basis for MFTF-B; LLNL, UCID-18496, Parts 1 and 2 (1980).
28. Grove, D.J., Meade, D.M.; Initial Studies of Confinement, Adiabatic Compression, and Neutral-Beam Heating in TFTR; Nucl. Fusion, Vol. 25, No. 9 (1985).
29. Porter, G.D., Ed.; TMX-U Final Report; UCID-20981, Vol. 1 & 2, February 1, 1988.
30. Wong, R.L., et al.; An Octopole Coil Configuration for the Tandem Mirror Experiment Upgrade; CH2251-7/86/0000-0231 (1986) IEEE.
31. MARS: Mirror Advanced Reactor Study Final Report; LLNL, UCRL-53480 (1984).
32. Hooper, E.B., Jr.; Octopole Anchor for Tandem Mirrors; UCID-20050, March 21, 1984, LLNL.
33. MINIMARS Conceptual Design: Final Report; J.D. Lee Ed.; UCID-20773, Vol. 1, September 1986.
34 Carlson, G.A.; et al.; Conceptual Design of the Field-Reversed Mirror Reactor; UCRL-52467, May 19, 1978.
35 Hoffman, A.L.; et al.; The Large-s Field-Reversed Configuration Experiment; Fusion Technology, Vol. 23, March 1993.
36. Miley, G.H.; Berk, H.L.; Cartwright, D.C.; Christy, R.F.; Hoffman, N.J.; Advanced Fusion Power; A Preliminary Assessment; National Research Council, Washington, DC; Report No.: AD-A185903/2/XAB, October 1987.
37 Teller, E.; et al.; Space Propulsion by Fusion in a Magnetic Dipole; Fusion Technology, Vol. 22, August 1992.
38 Chapman, R., Miley, G.H., Kernbichler, W., Heindler, M.; Fusion Space Propulsion with a Field Reversed Configuration; Fusion Technology, Vol. 15, 1989.
39 Hasegawa, A., et al.; A Description of a D-3He Fusion Reactor Based on A Dipole Magnetic Field; Fusion Technology, September, 1991.
40. Tsien, H.S.; "Takeoff from Satellite Orbits", Journal of the American Rocket Society, July-August, 1953.
41. Stuhlinger, E.; Ion Propulsion for Space Flight; NASA, McGraw Hill Book Co., 1964.
42. Irving, J.H; Low Thrust Flight: Variable Exhaust Velocity In Gravitational Fields; Chapter 10 in Space Technology, John Wiley and Sons, 1959.
43. Battin, R.H.; An Introduction to the Mathematics and Methods of Astrodynamics; New York, N.Y., American Institute of Aeronautics and Astronautics, 1987.
44. Vulpetti, G., private communication by FAX, p. 2, June 14, 1993.
45. Vulpetti, G.; Workshop for an Extra-Solar Mission: Identification, Feasibility & Planning; Technical Proposal, Rev. 1.0, November 1992.